

Dirac Magnetic Monopole Production from Photon Fusion in Proton Collisions

Triston Dougall¹ and Stuart D. Wick^{1,2}

¹ *Department of Physics,
Southern Methodist University
Dallas, TX 75275*

² *Department of Engineering Sciences & Applied Mathematics,
Northwestern University,
Evanston, IL 60201*

(Dated: June 05, 2007)

We calculate the lowest order cross-section for Dirac magnetic monopole production from photon fusion ($\gamma\gamma$) in $p\bar{p}$ collisions at $\sqrt{s} = 1.96$ TeV, pp collisions at $\sqrt{s} = 14$ TeV, and we compare $\gamma\gamma$ with Drell-Yan (DY) production. We find the total $\gamma\gamma$ cross-section is comparable with DY at $\sqrt{s} = 1.96$ TeV and dominates DY by a factor $\gtrsim 50$ at $\sqrt{s} = 14$ TeV. We conclude that both the $\gamma\gamma$ and DY processes allow for a monopole mass limit $m > 370$ GeV based upon the null results of the recent monopole search at the Collider Detector at Fermilab (CDF). We also conclude that $\gamma\gamma$ production is the leading mechanism to be considered for direct monopole searches at the Large Hadron Collider (LHC).

PACS numbers: 14.80Hv

I. INTRODUCTION

Magnetic monopoles have been a theoretical curiosity since the founding of electromagnetic theory and have motivated numerous innovative experimental searches. Maxwell’s equations possess a dual, electric–magnetic symmetry that goes unrealized without the discovery of magnetic charges. Stronger motivation for monopole searches was provided by Dirac who showed that the existence of a single magnetic monopole is sufficient to explain the observed quantization of electric charge [1], an empirical fact which goes otherwise unexplained. Magnetic monopoles are also present in a majority of grand unified theories (GUT) of particle interactions where monopoles are produced as topological defects during the GUT phase transition [2]. Consequently, if a GUT were realized in the early universe, after an era of inflation, then a population of magnetic monopoles would be left over as relics of the Big Bang [3].

Decades of interest in monopoles has inspired monopole searches in a wide range of physical settings [4]. It has been proposed that relativistic monopoles could be observed as a component of the cosmic rays [5] and recent flux limits have been reported [6] employing these techniques. Monopoles searches have been conducted in exotic materials like moon rocks [7] and terrestrial materials exposed to excessive radiation [8]. Collider searches for directly produced monopoles have been performed, most recently [9, 10]. Despite all efforts to date there are no definitive signals for the existence of magnetic monopoles.

The quantization of angular momentum for magnetic and electric poles yields the Dirac quantization condition, $eg = n/2$ (setting $\hbar = c = 1$) for electric and magnetic charges e and g , respectively. The magnetic charge

$$g = \frac{1}{2e} = \left(\frac{e}{2\alpha}\right) \simeq (68.5)e \quad (1)$$

is large in units of the electric charge (where we choose $n = 1$ and define $\alpha \equiv e^2 \simeq 1/137$). The large monopole charge implies a strong monopole–photon coupling, a characteristic of magnetic monopoles that will be exploited in this article.

A useful theory of monopole interactions does not currently exist to perform direct production calculations. The large monopole–photon coupling precludes the use of perturbation theory leaving us with a lowest order approximation as our only means to proceed. Previous authors [8–11] have employed a minimal model of monopole interactions which assumes a monopole–photon coupling that is proportional to the monopole’s induced electric field $g\beta$ for a monopole moving with velocity $\beta = v/c$. We follow these authors and use this same minimal model in our photon fusion ($\gamma\gamma$) and Drell–Yan (DY) calculations that follow.

Monopole searches at colliders are restricted to Dirac–type monopoles (and antimonopoles), which are hypothesized to be fundamental particles dual to the electron (and positron). GUT monopoles are excluded in collider searches as they generally have too large a mass ($M \sim 100\Lambda_{\text{GUT}}$ where Λ_{GUT} is the GUT symmetry breaking scale) and their internal structure exponentially suppresses their production cross–section. Models of Dirac monopole production have relied extensively on the DY process in which a quark and antiquark ($q\bar{q}$) from interacting protons annihilate to produce a monopole–antimonopole pair ($m\bar{m}$). (For an extensive review of the Drell–Yan process see [12].) The CDF Collaboration at the Fermilab Tevatron recently reported the results of a search for the direct production of magnetic monopoles [10]. With no monopole events found, CDF sets a mass limit $m > 360$ GeV assuming DY production of monopoles. A particle collider that probes a new energy frontier, such as the Large Hadron Collider (LHC), will open up new physics possibilities including the potential for the discovery of magnetic monopoles. Future monopole searches are likely to be undertaken at the LHC and will require detailed simulations of monopole events based upon our best knowledge of the leading monopole production mechanisms. Anticipating this need we investigate DY production at the LHC and consider an alternative production mechanism, the $\gamma\gamma$ fusion process.

The $\gamma\gamma$ production cross–section of heavy leptons, $\gamma\gamma \rightarrow L^-L^+$, has been studied in comparison with DY in pp collisions at LHC energies [13]. The full $\gamma\gamma$ process includes the individual regimes of inelastic, semi–elastic, and elastic scattering. The lepton production cross–section in each regime was found to be of the same order of magnitude while the total $\gamma\gamma$ cross–section, the sum of the individual regimes, was found to be nearly 10^2 below the DY cross–section. We repeat the $\gamma\gamma$ calculations for monopole production which entails replacing e (for leptons) with $g\beta$ (for monopoles) that, in light of eq. (1), will lead to greatly enhanced cross–sections. The DY cross–section will also be enhanced for monopole relative to lepton production, however it remains to be seen which process will dominate.

We restrict our calculations to Dirac monopoles (hereafter “monopoles”), assumed to be spin 1/2 fermions of minimal charge, only consider electromagnetic interactions, and assume a monopole–photon coupling $g\beta$ for final state monopoles of velocity β . In Section (II) we describe the $\gamma\gamma$ and DY calculations and discuss their relative dominance for lepton versus monopole production. The details of the $\gamma\gamma$ and DY calculations, which have been widely reported in the literature, are presented in Appendix (V) for the case of monopole production. In Section (III) we present our results for $p\bar{p}$ collisions at $\sqrt{s} = 1.96$ TeV, discuss the monopole lower mass bound reported by CDF, give a mass limit based on our calculations, and present our results for pp collisions at $\sqrt{s} = 14$ TeV. Our concluding remarks are given in Section (IV).

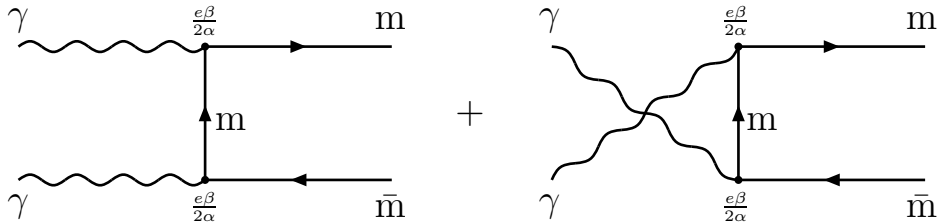


FIG. 1: The Feynmann diagrams for the $\gamma\gamma$ fusion subprocess which produce a monopole-antimonopole pair ($m\bar{m}$) in the final state. Two incoming virtual photons (γ) are radiated from the interacting protons or antiprotons (not shown). The virtual photons couple to the total charge distribution of the proton (during elastic scattering, which leaves the proton intact) or to a constituent quark within the proton (during inelastic scattering). The monopole-photon coupling is found from minimal assumptions of monopole interactions described in the text. The $\gamma\gamma$ cross-section formula for spin 1/2 monopoles is given in eq. (7).

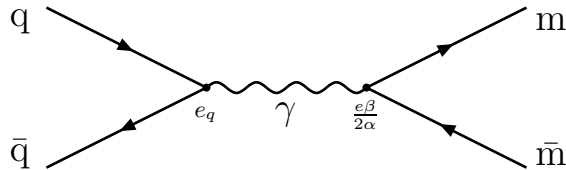


FIG. 2: The Feynmann diagram for the Drell-Yan subprocess which produces a monopole-antimonopole pair ($m\bar{m}$) in the final state. An incoming quark and antiquark ($q\bar{q}$), constituents of the colliding protons, annihilate into a virtual photon (γ) which then pair produces the final state monopoles. The DY cross-section formula for spin 1/2 monopoles is given in eq. (14).

II. PHOTON FUSION VERSUS THE DRELL-YAN PROCESS FOR MONOPOLE PRODUCTION

The $\gamma\gamma$ and DY processes for lepton production have been widely studied in proton collisions. The $\gamma\gamma$ subprocess for monopole production, depicted in Fig. (1), yields a monopole-antimonopole pair $m\bar{m}$ in the final state. The incident photons are radiated from the electric charge distribution of the colliding protons (or antiprotons). During elastic scattering the photon couples to the whole proton charge e and during inelastic scattering couples to constituent quarks of charge $e_q = \eta e$ where $\eta = 2/3(-1/3)$ for $q = u, c, t(d, s, b)$. We will compare $\gamma\gamma$ with the DY process (Fig. (2)) which dominates for lepton production. The full $\gamma\gamma$ and DY cross-section formulae are presented in Appendix (V) with the relevant couplings for monopole production.

To understand the relative strengths of $\gamma\gamma$ and DY production it is instructive to compare the electromagnetic couplings in the total cross-sections. For the estimates to follow we only consider quark-photon couplings $e_q = \eta e$ where $\eta = 2/3(-1/3)$ for $q = u, c, t(d, s, b)$. The full $\gamma\gamma$ calculation includes couplings to the whole proton charge which will provide a marginal increase to the $\gamma\gamma$ /DY enhancement we find in eq. (4) below. In the case of *lepton* production, $\gamma\gamma$ suppression relative to DY is anticipated merely by counting the powers of electromagnetic couplings in the total cross-sections. The ratio of electromagnetic couplings in the lepton production cross-sections for $\gamma\gamma$ relative to DY is

$$r_l = \frac{e_q^4 e^4}{e_q^2 e^2} = \bar{\eta}^2 \alpha^2 \quad (2)$$

where $\bar{\eta}$ is the average fractional quark charge contributing to the cross-section. Going from lepton to monopole production we simply replace $e \rightarrow g\beta = e\beta/2\alpha$ in the final state couplings (as shown in Figs. (1) and (2)). In this case the ratio of couplings is

$$r_m = \frac{e_q^4 \left(\frac{e\beta}{2\alpha}\right)^4}{e_q^2 \left(\frac{e\beta}{2\alpha}\right)^2} = \bar{\eta}^2 \frac{\beta^2}{4} \quad (3)$$

(where $\alpha \equiv e^2$). We can now estimate the change in the $\gamma\gamma$ /DY cross-section ratio expected for monopole versus

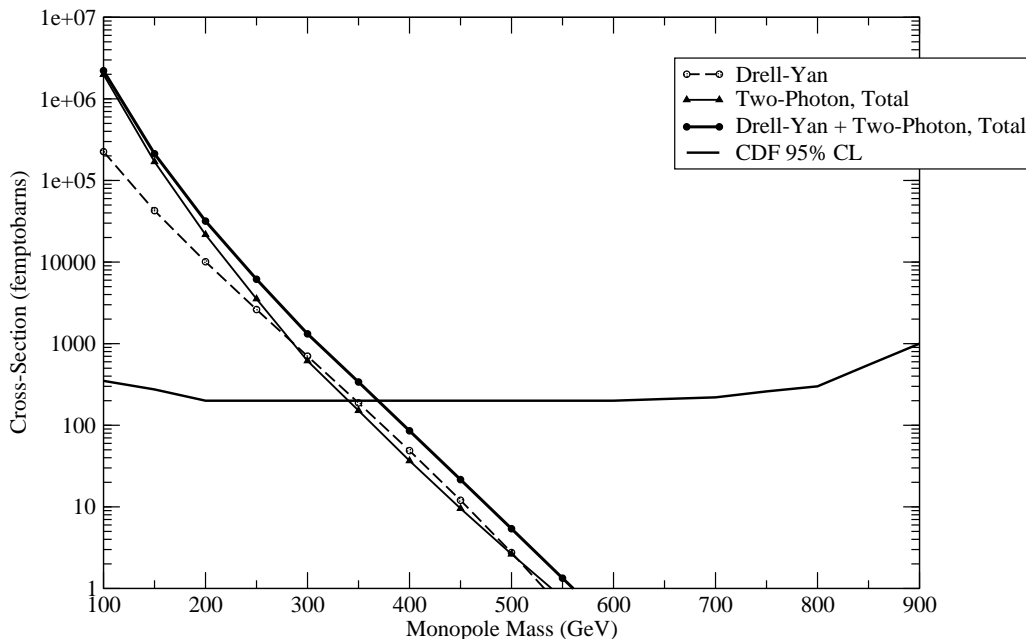


FIG. 3: The total cross-sections for $\gamma\gamma$ and DY production of monopoles in $p\bar{p}$ scattering vs. the mass of the produced monopole at $\sqrt{s} = 1.96$ TeV. The CDF reported cross-section limit at 95% confidence level (shown above) can be used to set a lower monopole mass limit assuming a production mechanism. The $\gamma\gamma$ and DY curves are nearly equal at the exclusion limit and independently call for a mass limits $m > 345$ GeV and $m > 350$ GeV, respectively. We also plot the sum of $\gamma\gamma$ and DY and find a monopole mass limit $m > 370$ GeV assuming both production mechanisms.

lepton production by taking a ratio of the ratios

$$R = \frac{r_m}{r_l} = \frac{\beta^2/4}{\alpha^2} \sim 4700 \quad (4)$$

setting $\beta = 1$. Drees, *et al.*, find $\gamma\gamma$ production of leptons to be nearly 10^2 below DY [13] for pp collisions at $\sqrt{s} = 14$ TeV, which implies a factor ~ 50 dominance of $\gamma\gamma$ over DY for monopole production assuming $\beta = 1$ in eq. (4). The effect of $\beta < 1$ for the production of slow moving monopoles is to be determined in our full calculation which follows.

III. MONOPOLE PRODUCTION IN PROTON COLLISIONS

We calculate $\gamma\gamma$ fusion for monopoles production following the formalism of Drees, *et al.* [13]. The detailed formulae are presented in Appendix (V) and full documentation of our $\gamma\gamma$ calculations is reported in a thesis of one of the authors [14]. Unlike the DY process, $\gamma\gamma$ production yields equivalent results in pp and $p\bar{p}$ scattering. The full $\gamma\gamma$ calculation includes contributions from three individual regimes; inelastic, semi-elastic, and elastic scattering, and we sum these individual regimes to find the total $\gamma\gamma$ cross-section. For inelastic scattering, $pp \rightarrow XX\gamma\gamma \rightarrow XXm\bar{m}$, both intermediate photons are radiated from partons (quarks or antiquarks) in the colliding protons. To approximate the quark distribution within the proton we use the Cteq6-1L parton distribution functions [15] and choose $Q^2 = \hat{s}/4$ throughout. Following [13], we employ an equivalent-photon approximation [16] for the photon spectrum of the intermediate quarks. In semi-elastic scattering, $pp \rightarrow pX\gamma\gamma \rightarrow pXm\bar{m}$, one intermediate photon is radiated from a quark, as in the inelastic process, while the second photon is radiated from the other proton, coupling to the total proton charge and leaving a final state proton intact. The photon spectrum associated with the interacting proton must be altered from the equivalent-photon approximation for quarks to account for the proton structure. To accommodate the proton structure we use the modified equivalent-photon approximation of [17]. For elastic scattering, $pp \rightarrow pp\gamma\gamma \rightarrow ppm\bar{m}$, both intermediate photons are radiated from the interacting protons leaving both protons intact in the final state.

The Fermilab Tevatron is a $p\bar{p}$ collider at center-of-mass energy $\sqrt{s} = 1.96$ TeV. We have calculated $\gamma\gamma$ and DY production of monopoles at the Tevatron and our results are presented in Fig. (3). The individual $\gamma\gamma$ scattering

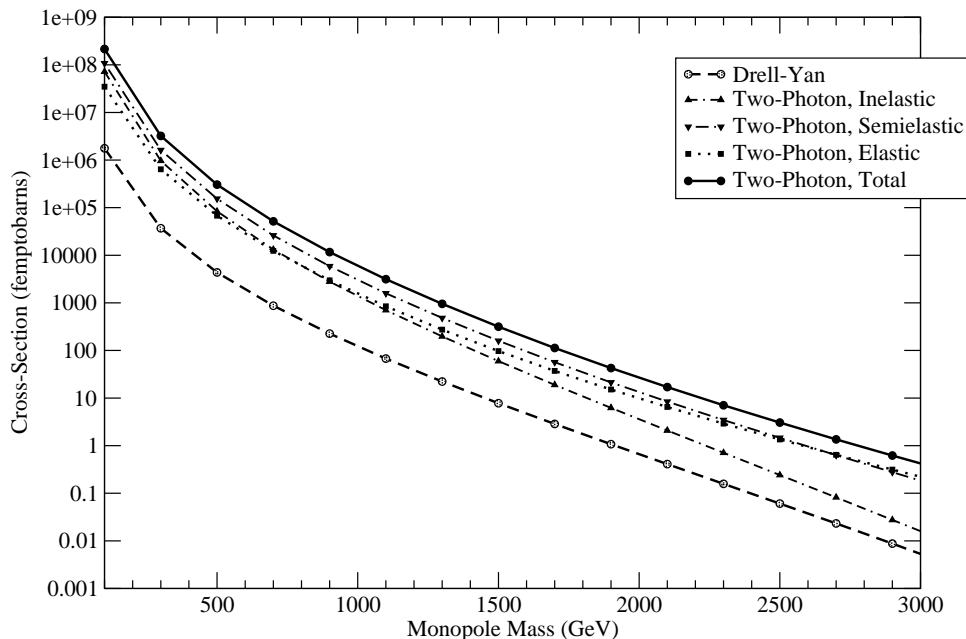


FIG. 4: The cross-sections for $\gamma\gamma$ fusion and DY processes in a pp interaction vs. the mass of the produced monopole at $\sqrt{s} = 14$ TeV. The $\gamma\gamma$ process is calculated in the elastic, semi-elastic and inelastic regimes shown above and the sum of the individual processes gives the total $\gamma\gamma$ production cross-section (solid line).

regimes are all of similar magnitude and happen to fall near the DY curve. To avoid cluttering Fig. (3) the individual regimes are not shown, but their contributions to the total $\gamma\gamma$ cross-section are roughly: inelastic (10%), semi-elastic (50%), and elastic (40%). The total $\gamma\gamma$ and DY cross-sections shown in Fig. (3) happen to be nearly equal over the range 300 to 500 GeV with $\gamma\gamma$ dominating at lower masses.

The result of a search for the direct production of monopoles was recently reported by the CDF Collaboration [10]. The search uses 35.7 pb^{-1} of CDF run II data where a special monopole trigger was employed. Monopole event simulations and conservative estimates of their experimental acceptance were used to establish a cross-section limit of approximately 200 femtobarns over a mass range 200 to 700 GeV at 95% confidence level based upon a lack of observed monopole events (see Fig. (3)). Assuming DY production of monopoles, CDF establishes a monopole mass limit of $m > 360$ GeV. Their monopole acceptance depends upon the production kinematics, but they estimate a limit in the total variation in acceptance to be less than 10% and conclude that mass limits from production mechanisms other than DY can be set with reasonable accuracy. Thus, we are justified in considering mass limits from $\gamma\gamma$ production based upon the CDF 95%CL limit.

The DY curve shown in Fig. (3) of [10] crosses the 95% CL limit near 360 GeV while our DY curve is slightly lower and crosses near 350 GeV. Therefore, our DY calculation calls for a slightly lower mass limit than CDF reports, but the addition of the $\gamma\gamma$ contribution to the DY production argues for an increase in the mass limit of 20 GeV to $m > 370$ GeV. See the $\gamma\gamma$ +DY curve in Fig. (3).

The LHC is designed to produce pp collisions copiously at $\sqrt{s} = 14$ TeV. The results of our calculations at LHC are presented in Fig. (4). We find that each of the individual $\gamma\gamma$ scattering regimes dominates DY by a factor $\gtrsim 10$ and the total $\gamma\gamma$ cross-section is a factor $\gtrsim 50$ larger than DY. Based upon our results we conclude that $\gamma\gamma$ fusion will be the leading mechanism for direct monopole production at LHC and argue for further investigation of the $\gamma\gamma$ process in detailed simulations of LHC monopole events.

If the LHC were to attain 100 fb^{-1} of integrated luminosity our calculations predict greater than 700,000 monopole events from $\gamma\gamma$ fusion for a monopole mass of 1 TeV. By comparison, the yield of 1 TeV monopoles from DY production is less than 15,000 events over the same period of time. The $\gamma\gamma$ process will allow LHC to extend their monopole search to relatively high masses. After collecting 100 fb^{-1} of data we predict in excess of 50 monopole events at monopole masses approaching 3 TeV.

IV. CONCLUSIONS

Motivated by recent monopole searches at the Fermilab Tevatron and the expectation of future monopole searches at the LHC we have calculated monopole production from the Drell–Yan and $\gamma\gamma$ fusion processes. We have compared these processes for both $p\bar{p}$ collisions at $\sqrt{s} = 1.96$ TeV and pp collisions at $\sqrt{s} = 14$ TeV. Our calculations are limited to a lowest order estimate assuming a monopole–photon coupling proportional to the induced electric field of a moving monopole. The monopole–photon coupling is strong for monopole velocities $\beta \sim 1$ which has prohibited our use of a perturbative expansion.

In $p\bar{p}$ collisions at the Tevatron we showed that the $\gamma\gamma$ total cross–section is approximately equal to DY in the mass range where the CDF collaboration sets a 95% confidence level cross–section limit. Based on our results, DY can be used set a mass limit $m > 350$ GeV and $\gamma\gamma$ can be used independently to set a mass limit $m > 345$ GeV. When both $\gamma\gamma$ and DY production are considered, the sum of the cross–sections implies the monopole mass limit of $m > 370$ GeV.

In pp collisions at the LHC we found that $\gamma\gamma$ fusion is the dominant production mechanism for magnetic monopoles by more than a factor 50 over the DY process. The inelastic, semi–elastic, and elastic regimes each dominate DY by a factor 10 or greater. We conclude that the $\gamma\gamma$ process should be considered the leading production mechanism for monopole searches at the LHC and emphasize the need for detailed studies of monopole events using the $\gamma\gamma$ process.

V. APPENDIX

Our $\gamma\gamma$ calculations follow the formalism and approximations of Drees *et al.*, [13]. We calculate inelastic, semi–elastic, and elastic processes and assume throughout this report that the final state monopoles are Dirac–type of minimal charged ($n = 1$), spin 1/2 fermions, and only consider their electromagnetic couplings. The $\gamma\gamma$ subprocess must satisfy the kinematic constraint $\hat{s} = (k_1 + k_2)^2 \geq 4m^2$ where k_1 and k_2 are the virtual photon four–momenta and the final state monopole pair has a total rest mass $2m$. We assume an effective photon approximation [16] to describe the photon spectrum of the interacting quark during inelastic scattering. The total cross–section for inelastic scattering is

$$\begin{aligned} \sigma_{pp}^{inel.}(s) = & \sum_{q, q'} \int_{4m^2/s}^1 dx_1 \int_{4m^2/sx_1}^1 dx_2 \int_{4m^2/sx_1x_2}^1 dz_1 \int_{4m^2/sx_1x_2z_1}^1 dz_2 e_q^2 e_{q'}^2 \\ & \cdot f_{q/p}(x_1, Q^2) f_{q'/p}(x_2, Q^2) f_{\gamma/q}(z_1) f_{\gamma/q'}(z_2) \hat{\sigma}_{\gamma\gamma}(x_1x_2z_1z_2s) \end{aligned} \quad (5)$$

where m is the monopole mass, $e_q = \eta e$ where $\eta = 2/3(-1/3)$ for $q = u, c, t(d, s, b)$, and $\hat{\sigma}_{\gamma\gamma}$ is the production subprocess cross–section with the center–of–mass energy $\sqrt{\hat{s}} = \sqrt{x_1x_2z_1z_2s}$. The structure function $f_{q/p}$ is the quark density inside the proton and $f_{\gamma/q}$ is the equivalent–photon spectrum of a quark. We use the Cteq6–1L parameterization of the parton densities [15] and chose the scale $Q^2 = \hat{s}/4$. With

$$f_{\gamma/q}(z) = f_{\gamma/q'}(z) = \frac{\alpha}{2\pi} \frac{(1 + (1 - z)^2)}{z} \ln(Q_{\max}^2/Q_{\min}^2) \quad (6)$$

where $Q_{\max}^2 = \hat{s}/4 - m^2$ and $Q_{\min}^2 = 1 \text{ GeV}^2$.

The final state monopole velocity is $\beta = (1 - 4m^2/\hat{s})^{1/2}$ for the subprocess center–of–mass energy $\sqrt{\hat{s}}$. The $\gamma\gamma \rightarrow m\bar{m}$ total cross–section is

$$\hat{\sigma}(\gamma\gamma \rightarrow m\bar{m}) = \frac{\pi\beta^5}{4\alpha^2\hat{s}} \left[\frac{3 - \beta^4}{2\beta} \ln \frac{1 + \beta}{1 - \beta} - (2 - \beta^2) \right]. \quad (7)$$

where $g^4\beta^4 = \beta^4/16\alpha^2$ using the Dirac quantization condition. The factor α^{-2} will be cancelled by two powers of α from eqs. (6) and (9).

The semi–elastic cross section for $pp \rightarrow m\bar{m}pX$ is given by

$$\begin{aligned} \sigma_{pp}^{semi-el.}(s) = & 2 \sum_q \int_{4m^2/s}^1 dx_1 \int_{4m^2/sx_1}^1 dz_1 \int_{4m^2/sx_1z_1}^1 dz_2 e_q^2 f_{q/p}(x_1, Q^2) \\ & \cdot f_{\gamma}(z_1) f_{\gamma/p}^{el.}(z_2) \hat{\sigma}_{\gamma\gamma}(x_1z_1z_2s) \end{aligned} \quad (8)$$

The subprocess energy now is given by $\sqrt{\hat{s}} = \sqrt{sx_1z_1z_2}$.

For the elastic photon spectrum $f_{\gamma/p}^{el.}(z)$ we use an analytic expression from [17] given by

$$f_{\gamma/p}^{el.}(z) = \frac{\alpha}{2\pi z} (1 + (1-z)^2) \left[\ln A - \frac{11}{6} + \frac{3}{A} - \frac{3}{2A^2} + \frac{1}{3A^3} \right], \quad (9)$$

for

$$A = 1 + \frac{0.71(\text{GeV})^2}{Q_{\min}^2}, \quad (10)$$

and where

$$Q_{\min}^2 = -2m_p^2 + \frac{1}{2s} \left[(s + m_p^2)(s - zs + m_p^2) - (s - m_p^2) \sqrt{(s - zs - m_p^2)^2 - 4m_p^2 zs} \right]. \quad (11)$$

At high energies Q_{\min}^2 is approximately $m_p^2 z^2 / (1-z)$.

The purely elastic scattering cross-section where both protons remain intact in the final state is

$$\sigma_{pp}^{el.}(s) = \int_{4m^2/s}^1 dz_1 \int_{4m^2/z_1 s}^1 dz_2 f_{\gamma/p}^{el.}(z_1) f_{\gamma/p}^{el.}(z_2) \hat{\sigma}_{\gamma\gamma}(\hat{s} = z_1 z_2 s). \quad (12)$$

In the DY process the annihilating $q\bar{q}$ pair must satisfy $\hat{s} = (p_1 + p_2)^2 \geq 4m^2$, for quark four-momenta p_1 and p_2 , to produce a final state monopole pair of total rest mass $2m$. The Drell-Yan cross-section for monopole production is

$$\sigma_{pp}^{\text{DY}}(s) = \sum_q \int_{4m^2/s}^1 dx_1 \int_{4m^2/x_1 s}^1 dx_2 f_{q/p}(x_1) f_{\bar{q}/p}(x_2) \hat{\sigma}_{q\bar{q}}(\hat{s} = x_1 x_2 s) \quad (13)$$

for the DY subprocess

$$\hat{\sigma}(q\bar{q} \rightarrow m\bar{m}) = \frac{\pi\eta^2\beta^3}{12\hat{s}} \left[2 - \frac{2}{3}\beta^2 \right] \quad (14)$$

where η is the fractional quark charge in units of e and the quark sum ranges from $\bar{t}, \bar{b}, \dots, b, t$, ensuring that only quarks and antiquarks of the same flavor contribute.

Acknowledgments

T. D. acknowledges research support from SMU's Dedman College. Both authors acknowledge useful discussions with Randall Scalise, Ryzsard Stroynowski, and Jingbo Ye.

-
- [1] P. A. M. Dirac, Proc. R. Soc. A **133**, 60 (1931).
[2] G. 't Hooft, Nucl. Phys. B **79**: 276-284 (1974); A. M. Polyakov, JETP Lett. **20**: 194-195 (1974); A. M. Polyakov, Pisma Zh. Eksp. Teor. Fiz. **20**:430-433 (1974).
[3] T. W. B. Kibble, Phys. Rept. **67**: 183 (1980).
[4] G. Giacomelli, *et al.*, [hep-exp/0005041].
[5] S. D. Wick, T. W. Kephart, T. J. Weiler, P. Biermann, Astro.Part.Phys. **18**: 663-687 (2003).
[6] D. Besson, [astro-ph/0611365].
[7] R. R. Ross, *et al.*, Phys. Rev. D **8**, 698 (1973).
[8] G. R. Kalbfleish *et al.*, Phys. Rev. Lett **85**, 5292 (2000); G. R. Kalbfleish *et al.*, Phys. Rev. D **69**, 052002 (2004).
[9] M. J. Mulhearn, "A Direct Search for Dirac Magnetic Monopoles," FERMILAB-THESIS-2004-51.
[10] CDF Collaboration, Phys. Rev. Lett **96**, 201801 (2006).
[11] G. Bauer, *et al.*, Nucl. Instrum. Meth. A **545**: 503-515 (2005).
[12] R. Stroynowski, Phys. Rept. **71**, 1 (1981).
[13] M. Drees, *et al.*, Phys. Rev. D **50**, 2335 (1994).
[14] T. Dougall, "Monopole Pair Production via Photon Fusion," M.S. Thesis, SMU-HEP-06-12, Dec. 2006.
[15] The Cteq6 parton distribution functions and documentation can be found at [http://www.phys.psu.edu/~cteq/].
[16] E. J. Williams, Phys. Rev. **45** (1934) 729(L); C. F. Weizsaecker, Z.Phys. **88** (1934) 612.
[17] M. Drees and D. Zeppenfeld, Phys. Rev. D **39**, 2536 (1989).